

2004

# An Experimental Study on Performance of Automotive Condenser and Evaporator

Seong Yeon Yoo  
*Chungnam National University*

Dae Woong Lee  
*Halla Climate Control Co.*

Follow this and additional works at: <http://docs.lib.purdue.edu/iracc>

---

Yoo, Seong Yeon and Lee, Dae Woong, "An Experimental Study on Performance of Automotive Condenser and Evaporator" (2004).  
*International Refrigeration and Air Conditioning Conference*. Paper 641.  
<http://docs.lib.purdue.edu/iracc/641>

This document has been made available through Purdue e-Pubs, a service of the Purdue University Libraries. Please contact [epubs@purdue.edu](mailto:epubs@purdue.edu) for additional information.

Complete proceedings may be acquired in print and on CD-ROM directly from the Ray W. Herrick Laboratories at <https://engineering.purdue.edu/Herrick/Events/orderlit.html>

# AN EXPERIMENTAL STUDY ON PERFORMANCE OF AUTOMOTIVE CONDENSER AND EVAPORATOR

Seon-Yeon Yoo<sup>1</sup>, Dae-Woong Lee<sup>2</sup>

<sup>1</sup>Chungnam National University, Department of Mechanical Design Engineering,  
Daejeon, 305-764, Korea  
Phone. +82-42-821-6646, Fax. +82-42-822-7366, E-mail. syyooh@cnu.ac.kr

<sup>2</sup>Halla Climate Control Corp., R & D Center,  
Daejeon, Korea  
Phone. +82-42-930-6703, Fax. +82-42-930-6619, E-mail. dwlee@mail.hcc.co.kr

## ABSTRACT

In this study, parallel flow condenser and laminated evaporator for automotive air-conditioning system are modified to improve performance. Gas-liquid separation type condenser in which condenser and receiver drier are integrated and one-tank laminated type evaporator have been developed, and then performances are investigated experimentally using HFC-134a. Heat transfer characteristics in the condenser are examined by means of air temperature, air velocity entering the condenser and the inlet pressure of refrigerant, and heat transfer characteristics in the evaporator are examined by means of air temperature, relative humidity, flow rate of air, outlet pressure of refrigerant and superheat. Pressure drops for both evaporator and condenser are also measured, and correlations for pressure drop are derived for condenser and evaporator, respectively.

## 1. INTRODUCTION

Automotive air conditioning system is usually installed in the limited space. So, compactness and relatively higher performance are required for the successful design of automotive heat exchanger. Early evaporator and condenser in automotive air conditioning system were fin-tube type. Recently, evaporator has been transformed from serpentine type to laminated type, and condenser has been changed from serpentine type to parallel flow type. Parallel flow type condenser with louvered fins has been developed to achieve higher performance compared to the fin & tube or serpentine type condenser (Sugihara and Lukas, 1990). Experimental study on the heat transfer and friction characteristic of air side has been performed by Sahnoun *et al.* (1992). Webb *et al.* (1995) conducted different experiments on 32 copper-brass and 27 aluminum heat exchangers and established equation for heat transfer and frictional coefficient. Ali *et al.* (1995) suggested improvements through pressure drop and heat transfer modeling for parallel flow type condenser (i.e. separated inlet, middle and outlet area). It was reported that outlet area should be 30 to 60% of inlet area to achieve the lowest pressure drop and higher heat transfer. Masafumi (1994) established heat transfer characteristics for multi channel tubes (4 to 30) condenser with different heights and widths of the channel. Multi channel tube condenser has smaller hydraulic diameter for the tubes with reduced charge quantity of refrigerant and can be produced through extrusion. These kinds of condensers are widely used in the automotive air conditioning system. And to add to that in multi channel tubes, Yamanaka *et al.* (1997) introduced sub-cooled condenser, which gives increased condensing efficiency by 5% and reduced power consumption by 10% as a result of auxiliary cooling mechanism at condenser outlet.

Laminated type evaporator introduced by Kurosawa *et al.* (1987). Ohara *et al.* (1988) reported forced convection heat transfer and two phase flow characteristics using CFC-12 for laminated evaporator with transverse slit shape. Ohara *et al.* (1990) also conducted a experimental test to establish relation between pressure drop and heat transfer characteristics at smooth wall and transverse rib shape plate. He found that heat transfer at transverse rib is about three times higher than smooth wall. Kaviani (1993) studied pressure drop and heat transfer characteristics for slit shape rib laminated plate with U-turn flow and HFC-134a. Kang (1995) carried out experiments on elliptic dimple laminated plate at various test conditions, vapor quality, mass velocity of refrigerant and amount of refrigerant oil quantity.

In this study, parallel flow condenser and laminated evaporator are modified to improve performance. Gas-liquid separation type condenser in which condenser and receiver drier are integrated and one-tank laminated type evaporator have been developed. Performances of the gas-liquid separation type condenser and the one-tank laminated type evaporator for automotive air conditioning system are investigated experimentally using HFC-134a. From experimental data such as air temperature, flow rate of air, relative humidity, refrigerant pressure and temperature, overall heat transfer coefficient are calculated for both condenser and evaporator, respectively. And pressure drop is correlated as a function of Reynolds number based on refrigerant mass flow rate and hydraulic diameter.

## 2. EXPERIMENTAL APPARATUS AND CONDITIONS

### 2.1 Condenser and Evaporator calorimeter

Experimental apparatus(calorimeter) shown in Fig. 1 consists of test section, condenser control section, evaporator control section, air heating system, air cooling system and control panel. The calorimeter has guide blades which make uniform air flow, and is insulated from environment. Heat gain and the heat loss by radiation are compensated for accurate measurement. Air heating system has a closed electric heater which can heat the circulated air more regularly than open type electric heater. Air cooling system is controlled by 30 HP compressor, expansion valve and evaporator pressure regulator. Two oil separators are installed in series to minimize performance error due to compressor oil. Oil is circulated less than 3% of refrigerant mass flow. Temperature is measured at inlet and outlet of experimental apparatus by RTD sensor. Brandt B-NZP1000 nozzles having diameter of 10 cm and 30 cm are used to measure low and high flow rate of air, respectively. 180 °C steam is supplied to the chamber to control humidity, and chilled mirror type humidity sensor which can calculates air enthalpy difference is used. Flow rate of refrigerant is measured using mass flow meter.

### 2.2 Experimental conditions

In case of gas-liquid separation type condenser, heat transfer and pressure drop phenomenon is somewhat different from those of conventional multi channel type condenser, because refrigerant flow through the condenser is divided into upper and lower part at the same time. As shown in Table 1, experimental conditions are considered for air side and refrigerant side, such as air velocity, air temperature, and refrigerant pressure of condenser inlet.

In case of laminated type evaporators, performance depends on number, length and angle of dimple or rib. Heat transfer and pressure drop characteristics are very sensitive to those conditions. In this study, for the successful design of slim laminated type evaporator with louver fin, experiments are performed by changing evaporator inlet

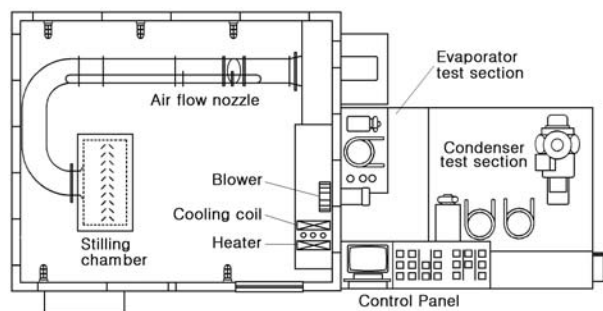


Figure 1: Schematic diagram of evaporator and condenser calorimeter

Table 1: Experimental conditions for condenser

|                                  |                  |
|----------------------------------|------------------|
| Air inlet temperature (°C)       | 30, 37           |
| Air inlet velocity (m/s)         | 2, 3, 4, 5       |
| Refrigerant inlet pressure (kPa) | 1474, 1739, 1867 |
| Super-heated temperature (°C)    | 25               |
| Sub-cooled temperature (°C)      | 5                |

Table 2: Experimental conditions for evaporator

|  |                    |
|--|--------------------|
| Air inlet temperature (°C)               | 25, 27, 30         |
| Air inlet relative humidity (%)          | 50, 60, 70         |
| Air volume flow rate (m <sup>3</sup> /h) | 300, 420, 500      |
| Refrigerant inlet pressure (kPa)         | 1621               |
| Refrigerant outlet pressure (kPa)        | 278, 297, 317, 356 |
| Super-heated temperature (°C)            | 5, 10              |

air temperature, relative humidity, air flow volume, evaporator outlet refrigerant pressure and superheat, as shown in Table 2.

### 3. RESULTS AND DISCUSSION

#### 3.1 Condenser

The measured pressure drop  $\Delta P$  for condenser is illustrated in Fig. 2. Pressure drop increases as the Reynolds number increases, in which Reynolds number is defined by gas viscosity of refrigerant as follows,

$$\text{Re}_g = \frac{G_r \cdot D_h}{\mu_g \cdot A} \quad (1)$$

where  $G_r$  is mass flow rate,  $D_h$  is hydraulic diameter of tubes,  $A$  is refrigerant flow area, and  $\mu_g$  is viscosity refrigerant gas. Experimental results are correlated using the least-square method as in Eq. (2).

$$\Delta P = 8 \times 10^{-7} \cdot \text{Re}_g^{1.8228} \quad (2)$$

The amount of heat transfer at condenser can be expressed in terms of LMTD(log mean temperature difference) and overall heat transfer coefficient and area, as in Eqs. (3) and (4),

$$Q = U \cdot A \cdot \Delta T_{LMTD} \quad (3)$$

$$\Delta T_{LMTD} = \frac{(T_{ri} - T_{ao}) - (T_{ro} - T_{ai})}{\ln\left(\frac{T_{ri} - T_{ao}}{T_{ro} - T_{ai}}\right)} \quad (4)$$

where  $U$  is overall heat transfer coefficient,  $A$  is heat transfer area, and subscript  $ri$ ,  $ro$ ,  $ai$  and  $ao$  indicate refrigerant inlet, refrigerant outlet, air inlet and air outlet temperature, respectively. The overall heat transfer coefficient of the condenser depends on geometric characteristics, Reynolds number inside the tube, and air velocity.

Figure 3 shows the variation of the overall heat transfer coefficient with the flow rate of refrigerant for various air velocities at superheat 25 °C and sub-cooling 5 °C. The overall heat transfer coefficient increases as refrigerant mass flow rate increases, and as the air velocity increases. Figure 4 shows the variation of overall heat transfer coefficient with air temperature entering the condenser, and refrigerant pressure at condenser inlet. Overall heat transfer coefficient has a tendency to increase at low condenser inlet pressure for same refrigerant flow rate because refrigerant vapor velocity at condenser decreases as pressure, temperature and density increase.

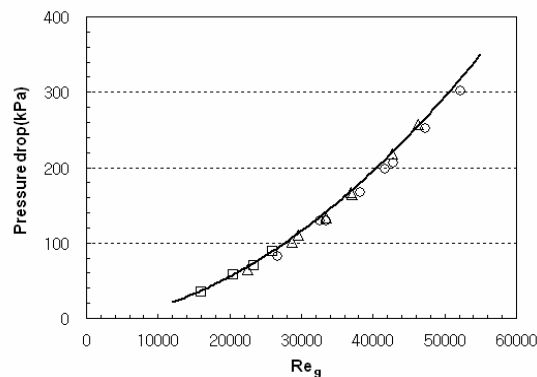


Figure 2: Variation of pressure drop with Reynolds number for condenser

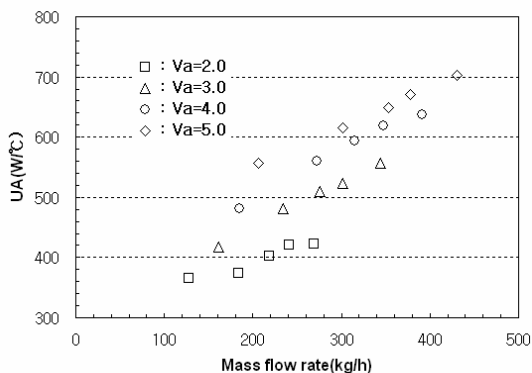


Figure 3: Variation of heat transfer coefficient with flow rate of refrigerant

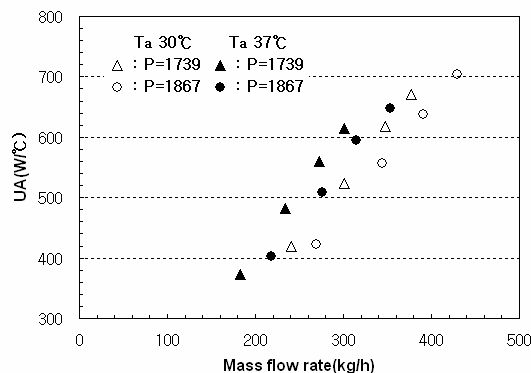


Figure 4: Variation of heat transfer coefficient with inlet pressure and air temperature

Variation of condensing capacity with air velocity at condenser front area is shown in Fig. 5 for various air temperatures and refrigerant pressures at condenser inlet. Condensing capacity is high at lower air temperatures and higher inlet pressure, and condensing capacity at 5 m/s air velocity is up to 40% higher than that at 2 m/s. Figure 6 presents the condensing capacity and pressure drop for various refrigerant flow passes inside the condenser at air velocity 5 m/s, superheat 25 °C and sub-cooling 5 °C. The sub-cooling region at condenser is limited within 14 to 17% of total area, superheating region by 36 to 42%, and two-phase region of upper condenser by 30 to 33% and that of lower condenser by 11 to 17%. Cooling capacity is not significantly influenced by the refrigerant flow pass. But Pressure drop has a tendency to increase as superheat region becomes larger, and sub-cooling region becomes smaller. Maximum difference in pressure drop is about 12%.

### 3.2 Evaporator

Variation of pressure drop with Reynolds number is presented in Fig. 7, in which Reynolds number is defined by

$$Re_g = \frac{x \cdot G_r \cdot D_h}{\mu_g \cdot A} \tag{5}$$

where  $A$  is refrigerant flow area, inlet refrigerant viscosity is calculated from refrigerant saturation vapor viscosity coefficient  $\mu_g$  and vapor quality ( $x$ ) at evaporator inlet.

Pressure drop increases as Reynolds number increases, and slope is clearly different for super-heat 5 °C and 10 °C. At the same Reynolds number, as superheat ( $T_{sh}$ ) increases, pressure drop also increases. Pressure drop  $\Delta P$  is correlated in terms of Reynolds number for each superheat as given in Eq. (6).

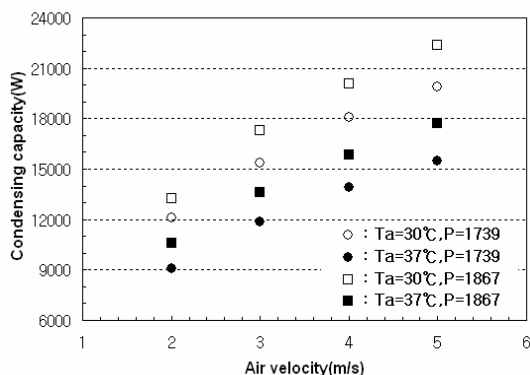


Figure 5: Variation of condensing capacity with air velocity

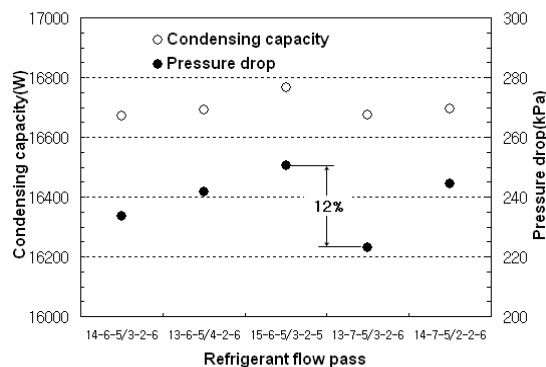


Figure 6: Condensing capacity and pressure drop for various refrigerant flow passes

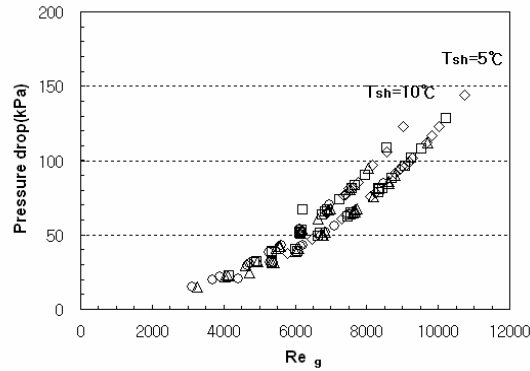


Figure 7: Variation of pressure drop with Reynolds number for evaporator

$$\Delta P = 2 \times 10^{-17} \cdot \text{Re}_g^{1.8241} \quad (\text{for } 10^\circ \text{C}) \quad (6)$$

$$\Delta P = 2 \times 10^{-17} \cdot \text{Re}_g^{1.9248} \quad (\text{for } 5^\circ \text{C})$$

In normal working conditions, evaporator surface is almost covered with condensation water film due to dehumidification process. Therefore, LMED(log mean enthalpy difference) is used to define overall heat transfer coefficient (Chiou *et al.*, 1994 and Lee *et al.*, 1996).

$$Q = U \cdot A \cdot \Delta h_m \quad (7)$$

$$\Delta h_m = \frac{(h_{ao} - h_{ria}) - (h_{ai} - h_{rsa})}{\ln\left(\frac{h_{ao} - h_{ria}}{h_{ai} - h_{rsa}}\right)} (1 - f_e) + \frac{(h_{ao} - h_{rsa}) - (h_{ai} - h_{roa})}{\ln\left(\frac{h_{ao} - h_{rsa}}{h_{ai} - h_{roa}}\right)} \cdot f_e \quad (8)$$

$$f_e = \frac{h_{ro} - h_{rs}}{h_{ro} - h_{ri}} \quad (9)$$

$h_{ai}$  and  $h_{ao}$  represent enthalpy of inlet air and outlet air, the terms of  $h_{ria}$ ,  $h_{rsa}$ , and  $h_{roa}$  are saturation wet air-enthalpies which are obtained at inlet, saturation and outlet refrigerant temperatures and the terms of  $h_{ro}$ ,  $h_{rs}$  and  $h_{ri}$  mean, outlet refrigerant enthalpy, saturation vapor enthalpy and inlet refrigerant enthalpy, respectively.  $f_e$  is defined as ratio of evaporation capacity at superheated state to the total evaporation capacity.

Variation of overall heat transfer coefficient with flow rate of air is shown in Fig. 8, in which superheats are 5 °C and 10 °C, ambient temperature is 25 °C and relative humidity is 50%. Overall heat transfer coefficient increases with the increase of air flow rate, and with the decrease of superheat and evaporation pressure. In low flow rate, the superheat effect is small, but the effect is significant in case of high flow rate. The humidity effect on the overall heat transfer coefficient for evaporator is presented in Fig. 9, where ambient temperature is 25 °C and air volume flow is 420 m<sup>3</sup>/h. Overall heat transfer coefficient increases as relative humidity increases, and the same effects for superheat and evaporator outlet pressure are seen as in Fig. 8. Figure 10 shows variation of overall heat transfer coefficient with ambient temperature, in which flow rate of air is 420 m<sup>3</sup>/h and relative humidity is 50%. Heat transfer coefficient increases as ambient temperature increases.

Figure 11 presents the variation of cooling capacity with air flow rate at 25 °C ambient temperature, and 50% relative humidity. Cooling capacity increases as the air flow increases, and this is attributed to the increased refrigerant mass flow as a result of higher convection heat transfer at higher air velocity. Cooling capacities in superheat 5 °C is higher than those in superheat 10 °C. Variation of cooling capacity with relative humidity is shown in Fig. 12. The cooling capacity at relative humidity of 70% is 23% higher than that at relative humidity of 50%. High relative humidity causes high air temperature across the evaporator, and consequently high refrigerant flow

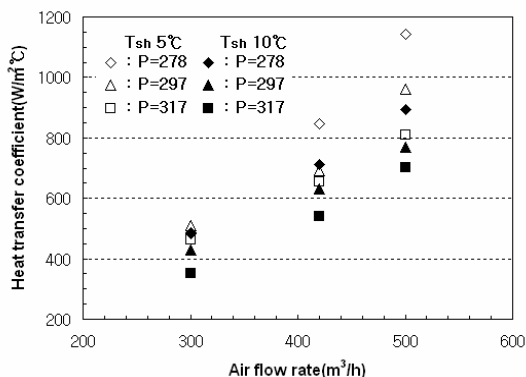


Figure 8: Variation of heat transfer coefficient with air flow rate ( $T_a=25\text{ }^\circ\text{C}$ ,  $R_h=50\%$ )

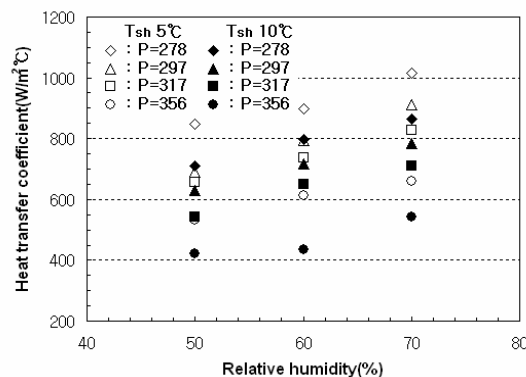


Figure 9: Variation of heat transfer coefficient with relative humidity ( $T_a=25\text{ }^\circ\text{C}$ ,  $Q_a=420\text{m}^3/\text{h}$ )

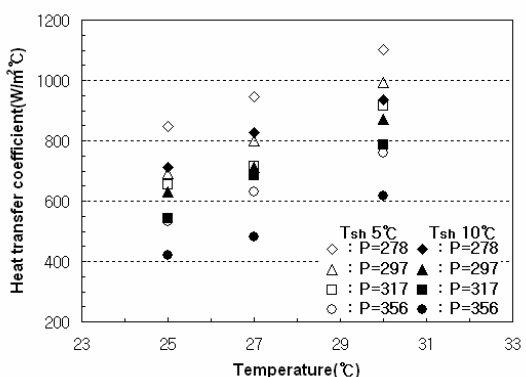


Figure 10: Variation of heat transfer coefficient with ambient temperature ( $Q_a=420\text{m}^3/\text{h}$ ,  $R_h=50\%$ )

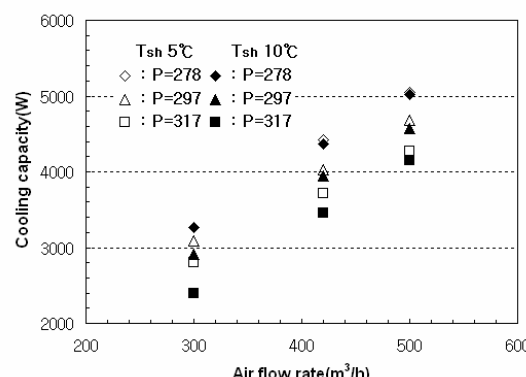


Figure 11: Cooling capacity vs. relative air flow rate ( $T_a=25\text{ }^\circ\text{C}$ ,  $R_h=50\%$ )

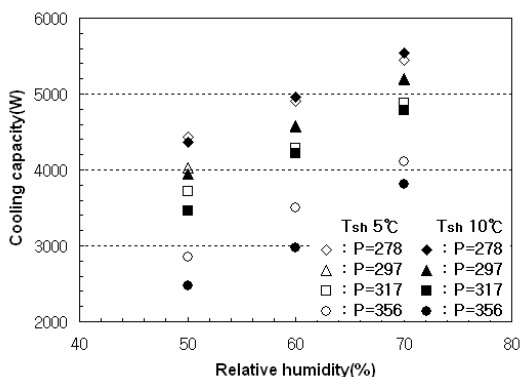


Figure 12: Cooling capacity vs. relative humidity ( $Q_a=420\text{m}^3/\text{h}$ ,  $T_a=25\text{ }^\circ\text{C}$ )

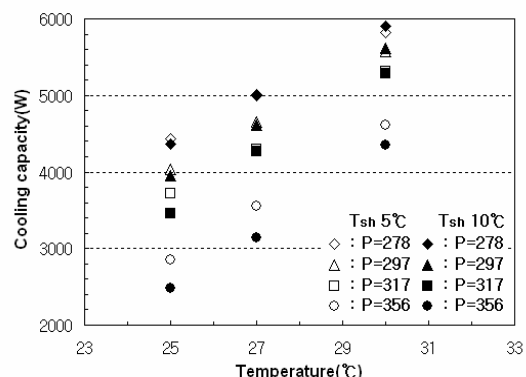


Figure 13: Cooling capacity vs. ambient temperature ( $Q_a=420\text{m}^3/\text{h}$ ,  $R_h=50\%$ )

rate. Figure 13 shows variation of cooling capacity with ambient temperature. As seen in the figure, cooling capacity at  $30\text{ }^\circ\text{C}$  ambient temperature is 25% higher than that at  $25\text{ }^\circ\text{C}$  ambient temperature.

#### 4. CONCLUSION

Gas-liquid separation type condenser, and one-tank laminated type evaporator is developed, and heat transfer and pressure drop characteristics were investigated experimentally. Major results of this study are as follows.

- Correlations for pressure drop are derived in terms of Reynolds number using the least-square fitting of experimental data.
- For condenser, air velocity and mass flow rate of refrigerant are main effect on overall heat transfer coefficient, and air temperature and inlet pressure of refrigerant slightly affect overall heat transfer coefficient.
- For condenser, cooling capacity is not significantly influenced by the refrigerant flow pass, but pressure drop increases as superheat region becomes larger.
- Overall heat transfer coefficient of evaporator increases as air flow rate, air temperature and relative humidity increases, but it decreases with increasing superheat and outlet pressure.

## REFERENCES

- Ali, A. A. R., Castro, F., Tinaut, F. V. and Melrar, M., 1995, Modeling of Automotive Air Conditioning Parallel flow Condenser with Pressure Drop Calculations, IMEche, Vol C496/020: p. 429-434.
- Chiou, C. B., Wang, C. C., Chang, Y. J. and Lu, D. C., 1994, Experimental Study of Heat Transfer and Flow Friction Characteristics of Automotive Evaporators, ASHRAE, Transactions, Vol. 100, Part 2.
- Kandlikar, S. G., 1990, A General Correlation for Saturated Two-phase Flow Boiling Heat Transfer inside Horizontal and Vertical Tubes, J. of Heat Transfer, Vol. 112, pp. 219-228.
- Kang, J. K., 1995, Evaporation Heat Transfer and Pressure Drop of HFC134a and PAG oil mixtures in a Ribbed Flat Channel for Plate/ Fin Type Evaporator, Ph. D. thesis, National Fisheries University of Pusan, Korea.
- Kaviany, M., 1993, Experimental Study of Pressure Drop and Heat Transfer in a Plate Evaporator, Ford Motor Co. Contract report. C1-24E
- Kurosawa, I., and Noguchi, I., 1987, Development on a High Efficiency Drawn Cup Type Evaporator Core, SAE, 870030.
- Lee, G. H., Jung, J. D. and Choi, K. H., 1996, System performance characteristics of an automotive air conditioner with variations of charging conditions, Proceedings of the SAREK 1996 Winter Annular Conference, p. 301-306.
- Lee, J. H., Jeon, C. D., Jeoung, J. W., and Lee, D. K., 1996, A Study of Pressure Drop and Heat Transfer Characteristics in the Multi-Channel Tube for Automotive Condenser, Halla Climate Control Co. Technical report, HCC-94DE.
- Masafumi Katsuta, 1994, The Effective of a Cross-Section Geometry on the Condensation Heat Transfer inside Multi-Pass Tube, Proc. WTPF, Vol. 2 pp. 146-157, AFERC, POSTECH.
- Ohara, T. and Takahashi, T., 1988, High Performance Evaporator Development, SAE 880047.
- Ohara, T., Yamamoto, T., and Fujita, H., 1990, Heat Transfer and Pressure Drop of Boiling Flow in a Cross-ribbed Flat Channel, Int. J. Heat and Mass Transfer, Vol. 17, pp. 555-566.
- Sugihara, A. and Lukas, H. G., 1990, Performance of Parallel flow Condensers in Vehicular Applications, SAE 900597.
- Sahnoun, A. and Webb, R. L., 1992, Prediction of Heat Transfer and Friction for Louver Fin Geometry, Transactions of the ASME, Vol. 114: p. 893-900.
- Webb, R. L., Chang, Y. J. and Wang, C. C., 1995, Heat Transfer and Friction Correlations for the Louver Fin Geometry, IMechE, Vol. C496/081: p. 533-541.
- Yamanaka, Y., Matsuo, H., Tuzuki, K., Tsuboko, T. and Nishimura, Y., 1997, Development of sub-cool System, SAE 970110.

## ACKNOWLEDGEMENT

This research was partially supported by the Regional Research Center for Advanced Climate Control Technology at Sun Moon University funded by KOSEF.